BUILD SIMUL (2015) 8: 701 – 709
DOI 10.1007/s12273-015-0248-1

Buoyancy-driven flow through a ceiling aperture in a corridor: A study on smoke propagation and prevention

Bosi Zhang[1], **Jiaqing Zhang**[2], **Shouxiang Lu**[1] (✉), **Changhai Li**[1]

1. State Key Laboratory of Fire Science, University of Science and Technology of China, Hefei, Anhui 230027, China
2. State Grid Anhui Electric Power Research Institute, Hefei, Anhui 230022, China

Abstract

Analyzing numerous computational fluid dynamics (CFD) simulations of a two-level corridor model, smoke propagation and prevention were investigated. In all simulations, the fire source was placed inside the lower corridor, which we refer to as the fire corridor. Results show that after smoke flows in through the ceiling aperture, a dangerous environment forms quickly in the upper corridor. The smoke layer in the upper corridor descends nearly to floor level through buoyancy and air flowing in through the doorways. The fire hazard created in the upper level is larger than that of the fire corridor. In regard to fire prevention, the effectiveness of a counter airflow at the ceiling aperture is demonstrated, and critical velocities for counter airflow are derived through CFD simulations. A simple model for predicting this critical velocity is proposed based on the Froude modeling. The critical Froude number initially declines linearly with the dimensionless distance between the fire source and the ceiling aperture, and then stabilizes at 0.38 when this distance is larger than 3.00. This model can be used for coarse design of the counter airflow smoke control system.

Keywords

smoke propagation,
smoke prevention,
counter airflow,
corridor,
ceiling aperture

Article History

Received: 10 March 2015
Revised: 12 July 2015
Accepted: 19 July 2015

1 Introduction

The majority of casualties from fires is caused by smoke inhalation of poisonous and high-temperature gases. Hence smoke propagation and smoke management is pivotal in fire safety research (Mowrer 2002; Chung et al. 2005; Zhu 2009). Corridors are common in buildings and always serve as escape routes. During fire outbreaks within buildings, the corridor environment is critical to the evacuation of personnel. In addition, the corridor usually connects many rooms. Therefore, the potential risk from smoke contamination not only comes from corridor fires, but may also come from fires occurring in other connected rooms. Moreover, smoke from corridor fires is liable to spread into other spaces and expands the area affected by smoke. To secure safe evacuation during a fire outbreak and limit the smoke contamination area, it is necessary to prevent smoke from flowing into the upper level. In some newly constructed modern buildings, underground buildings, substations, nuclear power plants, and ship structures, some of the levels are connected directly by stairways in the corridor instead of stairwells because of space limitations or impositions from the structure. In these buildings, smoke spreads into the upper level more quickly and results in a more dangerous environment there. Therefore, a study on how smoke propagation and prevention in multi-level corridors directly connected by stairways is warranted.

Smoke propagation in corridors has drawn considerable attention because the length-to-width ratio of corridors is quite large (Quintiere et al. 1978; Heskestad and Hill 1986; Matsuyama et al. 2001; Bailey et al. 2002; Hu et al. 2006a). Estimating temperature and velocity of smoke along the corridor was performed by Bailey et al. (2002), Hu et al. (2005), Delichatsios (1981), and Evers and Waterhouse (1978). Most of these studies confirmed that smoke temperature decreases exponentially along the length of the corridor. Bailey et al. (2002) proposed a power law function established from the results of large eddy simulations (LESs). This

---

E-mail: sxlu@ustc.edu.cn

correlation was adopted in the design of corridor flow submodel in the Consolidated Model of Fire and Smoke Transport (Bailey et al. 2002). The descent of fire smoke in the corridor was revealed experimentally by Kim et al. (1998). Smoke dispersions near the end of the corridor and an oscillatory behavior at the smoke layer interface were discussed in detail in their study. The mixing of the smoke and air layers in corridors was investigated in a study performed by Guo et al. (2009), and a modified fire zone model was developed. To summarize, the special characteristics of smoke propagation in corridors has been investigated. However, most studies have mainly focused on smoke propagation behavior in a single-floor corridor. To verify the accuracy of simulations or to explore the stack effect in the stairwell, smoke movement in the multi-level corridor model has been involved in some studies (Hua et al. 2005; Zhong et al. 2005; Hadjisophocleous and Jia 2009). In their tests models, the corridors were connected by a stairwell rather than stairways directly in the corridor. As mentioned before, the latter is prone to forming dangerous environments in the upper levels. Hence, smoke propagation in multi-level corridors connected by stairways requires a separate study, and a means to control smoke should also be explored.

The smoke management that we propose aims to prevent smoke from flowing out of the fire corridor through the ceiling aperture, i.e., the stairways in the corridor. This objective may be achieved by having stairways closed during fires. However, this measure is impractical if the stairways are to serve as main evacuation exits or rescue entrances during fire outbreaks. Counter airflow, which is a fundamental principle in smoke management, is possible at these openings (Havlovick et al. 2002). Moreover, counter airflow would be an effective method that considered both smoke management and personnel evacuation in fires. Buoyancy-driven smoke can be prevented from dispersing through the ceiling aperture when the inertial force of the airflow is sufficiently large to resist the buoyancy of smoke. Therefore, the critical velocity of the counter airflow is most crucial and central in this study. Previous studies estimate this critical velocity mainly focused on the type of counter airflow that is used for limiting smoke to a fraction of the fire space, such as for the longitudinal ventilation system in tunnels (Thomas 1968; Oka and Atkinson 1995; Kunsch 1998; Wu and Baker 2000). In studies by Heskestad and Spaulding (1991) and Ingason and Werling (2002), the counter airflow was used to prevent smoke from dispersing through the horizontal and vertical openings in the fire space. However, the fire source was located in a room rather than a corridor. Generally, smoke propagation in multi-level connected corridors has not received much attention, and counter airflow as prevention in stairways of corridors has not been studied.

In the present study, smoke propagation in a two connected corridors was investigated using CFD simulations with attention paid to the flow of smoke through the ceiling aperture and subsequent dispersal through the upper level. The effectiveness of forced airflow in managing smoke in the ceiling aperture was explored. Using numerous simulations with consideration of the effects of fire size and fire location, critical velocities required to prevent smoke dispersion from the fire corridor were obtained.

2 Simulation method

CFD modeling is effective in predicting thermal fluid phenomena involved in fires and is widely used in fire safety research (Chow 1996; Gong and Li 2010; Wang et al. 2011; Hu et al. 2014). The Fire Dynamics Simulator (FDS), which was developed by the National Institute of Standards and Technology, is a CFD software that is commonly adopted in fire-related research (Hu et al. 2008; Wang et al. 2011; Chiu et al. 2013). The LES of FDS (version 5) was used for all simulations.

The FDS modeling results for smoke movement, under different ventilation conditions in corridors and tunnels, which have similar geometric characteristics to corridors have been validated with the corresponding experimental results in several studies (Hu et al. 2007; Wu et al. 2013; Gottuk et al. 2008; Hu et al. 2006b). These results show that predictions of smoke movement in long corridors agreed well with those deduced from experiments, especially for the gas temperature and the velocity of smoke, which are of main interest. Moreover, the application of the FDS to smoke movement under forced airflow and critical velocity estimates for the forced airflow in smoke management have been confirmed (Roh et al. 2007; Lee and Ryou 2006). To summarize, the FDS is appropriate in studying smoke propagation and prevention in the two-level corridor.

An approximation of the Navier–Stokes equations appropriate for low-Mach-number applications is used in FDS. LES, the default solver in FDS, is used in all simulations. In LESs, the large-scale eddies are computed directly, whereas the dissipative processes at sub-grid scales are modeled (McGrattan et al. 2010). In using this sub-grid model, two aspects, the appropriate grid scale and appropriate parameters, need considering and are crucial to the accuracy of the results (Hu et al. 2008).

The range of the appropriate grid scales was calculated by adopting the methods recommended in the user's guide of the FDS, which evaluates the accuracy of the mesh using the non-dimensional expression D^*/δ_x. Here, δ_x is the nominal size of a mesh cell (m) and D^* is the characteristic fire diameter defined as (McGrattan et al. 2010).

$$D^* = \left(\frac{\dot{Q}}{\rho_\infty c_\mathrm{p} T_\infty \sqrt{g}}\right)^{2/5} \tag{1}$$

where $\dot{Q}$ is the heat release rate (HRR) of fire (kW), g is the acceleration of gravity (m/s^2), and c_p, T_∞, and ρ_∞ are the specific heat (J/(kg·K)), temperature (K), and density (kg/m^3) of ambient environment, respectively. The recommended values for D^*/δ_x range from 4 to 16. Depending on the range for mesh grids, an optimal size was obtained by employing mesh sensitivity analysis. Taking simulation accuracy and computational efficiency into consideration, a grid system with grid size of 0.05 m was finally selected.

For LES models, FDS uses the Smagorinsky form to model the sub-grid scale turbulence, and the most important coefficient in turbulence model is the turbulent viscosity, which is obtained using the constant-coefficient Smagorinsky model. The viscosity is defined as (McGrattan et al. 2010)

$$\mu_\mathrm{LES} = \rho(C_\mathrm{s}\Delta)^2\left(2\bar{S}_{ij} : \bar{S}_{ij} - \frac{2}{3}(\nabla\cdot\bar{u})^2\right)^{1/2} \tag{2}$$

The thermal conductivity and the material diffusivity, which are related to the viscosity, are defined as (McGrattan et al. 2010)

$$k_\mathrm{LES} = \frac{\mu_\mathrm{LES} c_\mathrm{p}}{Pr_\mathrm{t}}; \quad (\rho D)_{l;\mathrm{LES}} = \frac{\mu_\mathrm{LES}}{Sc_\mathrm{t}} \tag{3}$$

where the parameter C_s, the Prandtl number Pr_t, and the Schmidt number Sc_t are assumed constant, their recommended values being $C_\mathrm{s} = 0.2$, $Pr_\mathrm{t} = 0.5$, and $Sc_\mathrm{t} = 0.5$ (McGrattan et al. 2010).

The numerical simulation is applicable for investigating the smoke management with forced airflow (Hwang and Edwards 2005; Hu et al. 2008). To determine the critical velocity, the flow rate of the counter airflow is usually set sufficiently large to prevent smoke from flowing out at the outset. The flow rate is then decreased gradually until the first indication of smoke appears in the aperture (Heskestad and Spaulding 1991). Numerous runs are needed to obtain the critical velocity for each fire scenario. The consistency of the test conditions among these cases is crucial for the accuracy of the critical velocity. In this regard, given that the test condition is easier to control in simulations than in experimental tests, numerical simulations are most appropriate to calculate the critical velocity of the counter airflow. The direction of flow in the ceiling aperture is downward when the counter airflow works effectively in preventing smoke propagation. The reversal in the direction of this flow is considered an indicator that a critical velocity for a counter airflow is attained. The critical flow rate of the counter airflow is taken to determine an average value for the first flow rate indicating the presence of fire smoke and the preceding one (Heskestad and Spaulding 1991). The velocity of the counter airflow was calculated by dividing the critical volume rate of the counter airflow by the area of the ceiling aperture.

3 Physical model and fire scenarios

3.1 Physical model

The size of the two-level corridor was set to 20.00 m (L) × 2.40 m (W) × 5.00 m (H), as shown in Fig. 1. With dimensions of 1.85 m (H) × 1.00 m (W), the four doors at each of its ends were all kept open during the simulations. The fire corridor and the upper level were connected by a ceiling aperture of dimensions 1.20 m (L) × 1.00 m (W). The ceiling aperture was centered width-wise across the corridor, and close to Door 2. The distance between the fire source and the ceiling aperture is a key parameter and was varied by changing the location of the fire source in the corridor.

The measurement system for the simulation model is illustrated in Fig. 1. Two sets of measurement points located in the center of the fire corridor and the upper level, labeled T1 and T2, respectively, were sites where temperature was recorded. The highest measure point was located at 0.10 m under the ceiling, and the other measure points were vertically placed at a uniform spacing of 0.10 m. T1 and T2 were used to estimate the temperature field of smoke within the fire corridor and the upper level. Nineteen horizontal velocity measure points were evenly arrayed over Door 1 with vertical spacing 0.10 m; the points are denoted V1 and V2 in the fire corridor and the upper level, respectively. The horizontal velocities were used to calculate the height of the neutral plane of Door 1 in both levels. The location used to measure the height of the smoke layer was 1 m from Door 1, as shown in Fig. 1(a) and (b).

Predictably, the gas temperature was higher and mixing of air and smoke was stronger along the side of the ceiling aperture close to the fire source. This results in a greater probability of smoke flowing out along this side. Measurement points were therefore denser along the side close to the fire than for the opposite side of the ceiling aperture, as shown in Fig. 1(c). These measurement points were used to obtain the temperature of the smoke as it passes through the ceiling aperture.

For the scenarios regarding smoke management, the simulation area of the upper corridor far from the ceiling aperture was omitted to reduce computation times. The simulation zone of the upper corridor in these simulations is the gray area bounded with black dotted lines, as shown in Fig. 1. As there is no smoke flowing into the upper corridor in the critical condition, this simplification has no significant effect on the accuracy of the simulations and results obtained.

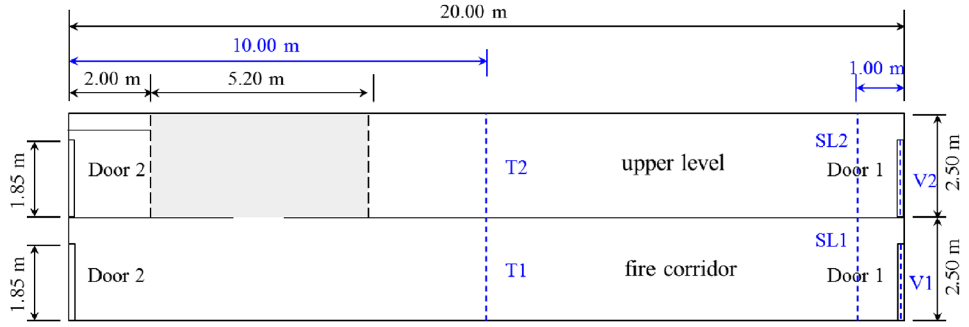

(a) Front view

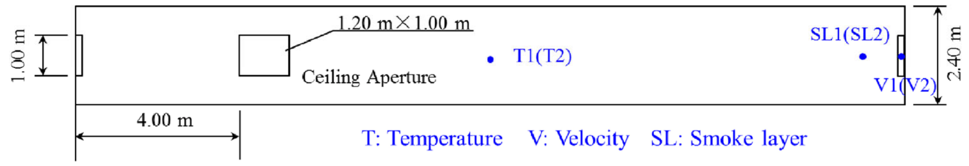

(b) Top view

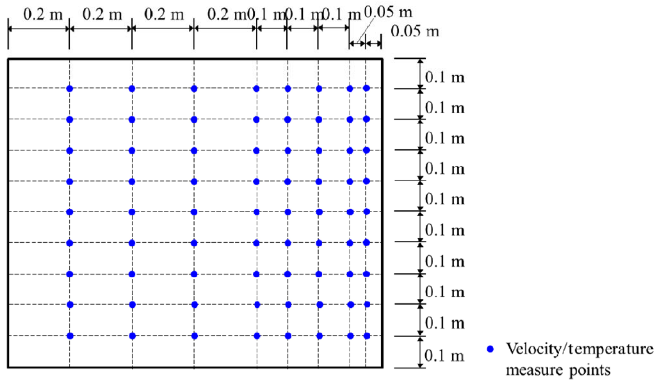

(c) Arrangement of measurement points over the ceiling aperture

Fig. 1 Schematic of the corridor and measurement system

A velocity boundary was set up in the ceiling of the upper level and served as the source of forced airflow during the simulations.

3.2 Simulation scenarios

Details of settings for each simulation scenario are listed in Table 1. The HRR of fires and the fire–aperture distance were the two factors considered that varied for the different scenarios. The HRRs were set to 200, 300, 500, 800, and 1000 kW. Seven fire–aperture distances were considered for each HRR. With a total of 35 scenarios, the total number of fire simulations performed was over 300. The fire for all simulations was steady fire with the HRR reached a set value after 1 s, and the duration of each simulation was set to 180 s.

Table 1 Details of settings for the different simulation scenarios

Case No.	Ventilation condition	Fire size (kW)	Distances between the fire source and the ceiling aperture (m)
1-1-1-7	No forced ventilation / counter airflow at the ceiling aperture	200	2; 2.5; 3; 4; 5; 7.5; 10
2-1-2-7		300	2; 2.5; 3; 4; 5; 7.5; 10
3-1-3-7		500	2; 2.5; 3; 4; 5; 7.5; 10
4-1-4-7		800	2; 2.5; 3; 4; 5; 7.5; 10
5-1-5-7		1000	2; 2.5; 3; 4; 5; 7.5; 10

4 Results and discussions

4.1 Smoke propagation in the two-level corridor

Smoke propagation in the two-level corridor model is illustrated using Cases 1-7 and 5-1 as examples; in particular their temperature distributions throughout the fire corridor and the upper level are given in Fig. 2. A distinct interface exists between the smoke layer and the air layer, and a strong stratification exists in the smoke layer of the fire corridor. The smoke layer almost descends to the floor level, and there is a distinct temperature gradient along the corridor height in the upper level. According to Zukoski (1986), the extent of stratification in the smoke layer depends greatly on the entrainment of the plume and the ceiling jet, and can be determined by the Richardson number, which is defined as

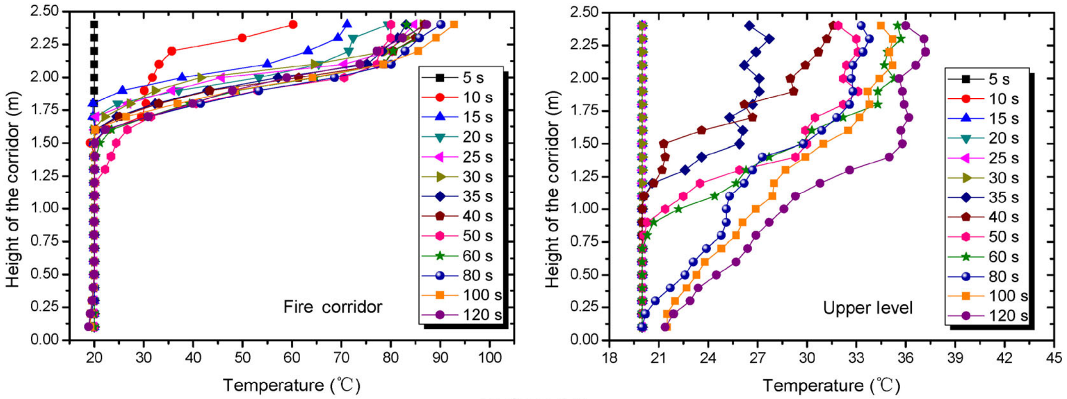

(a) Case 1-7

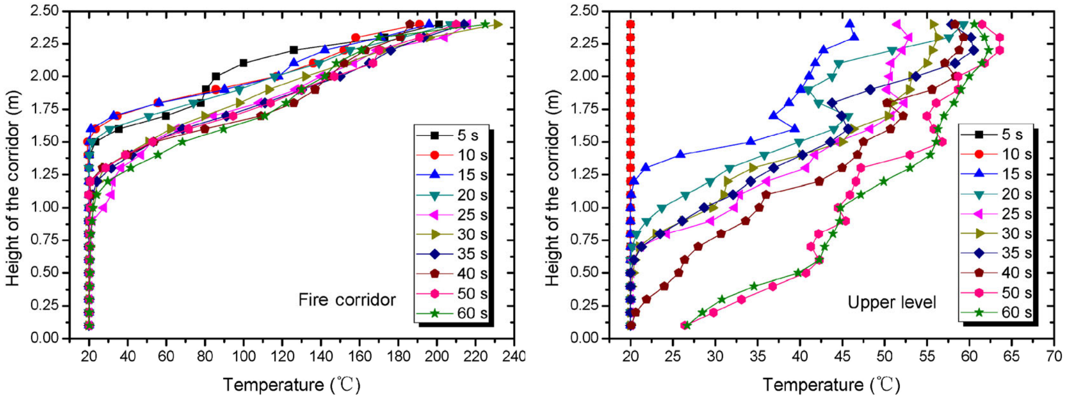

(b) Case 5-1

Fig. 2 Vertical profiles of gas temperatures in the fire corridor and upper level at various times during the simulation

the ratio of the buoyancy and the momentum of the smoke layer (Zukoski 1986):

$$Ri = \frac{\Delta\rho g\delta}{\rho_{\mathrm{c}} V_{\mathrm{c}}^2} \tag{4}$$

where $\Delta\rho = \rho_{\mathrm{a}} - \rho_{\mathrm{c}}$, and ρ_{a} is the density of air (kg/m^3), ρ_{c} is the density of ceiling jet (kg/m^3), g is the acceleration of gravity (m/s^2), and V_{c} is the characteristic velocity of the ceiling jet (m/s). Zukoski (1986) noted that the degree of entrainment into the smoke layer was inversely proportional to *Ri* of the ceiling jet, which increases with the square of the distance from the impingement point of the fire plume. If the distance from the impingement point is larger than the fire plume height, almost no entrainment occurs in the ceiling jet (Zukoski 1986). Therefore, a well-mixed smoke layer is hard to form in the corridor, and the temperature gradient always exists in the smoke layer. For the upper level, the ceiling jet formed by the plume-like flow can be regarded as a smoke flow that is extremely far from the fire source. Thus, this ceiling jet has a larger *Ri* value than the ceiling jet in the fire corridor. The above analysis is also supported by the vector velocity of the smoke flow in the fire corridor and the upper level, as shown in Fig. 3. From the local detailed images, the vertical velocity of the smoke is negligible compared with the horizontal velocity, indicating that entrainment is not significant in the two-level corridor.

As seen in Fig. 2, the smoke layer almost descends to the floor of the upper level, which results in a more dangerous fire environment in the upper level than in the fire corridor from the perspective of temperature distribution. One reason for this phenomenon is that the temperature of the plume-like flow is relatively low, and thus the smoke layer descends because of low buoyancy. Another reason is related to the flow through the two doors in the upper level. A comparison of the smoke layer height and the neutral plane height of Door 1 in the fire corridor and the upper level are shown in Fig. 4. The neutral plane height is correlated with the horizontal velocities measured in Door 1. Under steady state, the smoke layer and the neutral plane of Door 1 are located at almost the same height in the fire corridor. Hence, little of the smoke was blown back by inflow air from the door. Meanwhile, for the upper level, the smoke layer height is clearly lower than the neutral plane of Door 1. Thus the inflow air from the door entrained a considerable amount of fire smoke back toward the fire plume, as shown in Fig. 5. From Fig. 3, the interaction between the jet flow and the back flow was not significant

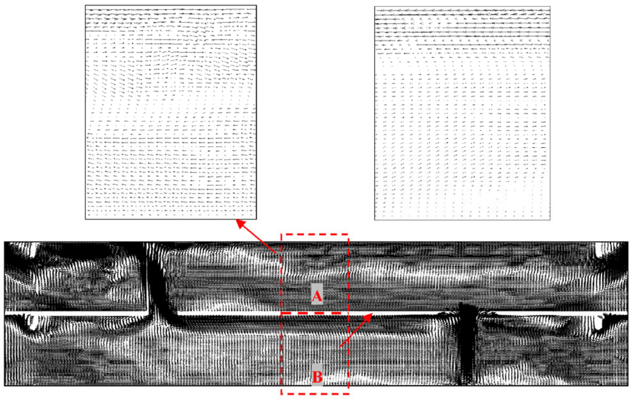

(a) Case 1-7 (*t* = 120 s)

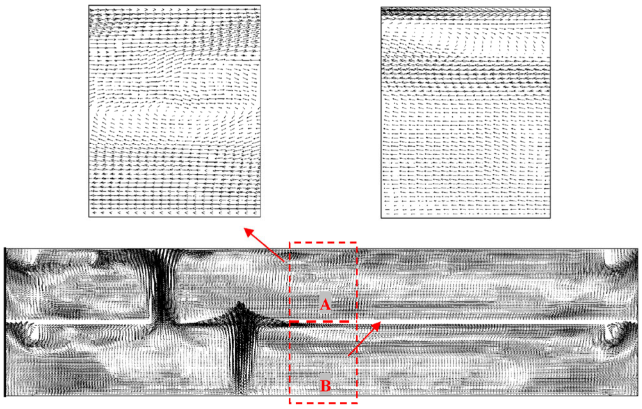

(b) Case 5-1 (*t* = 60 s)

Fig. 3 Profiles of vector velocities and local details

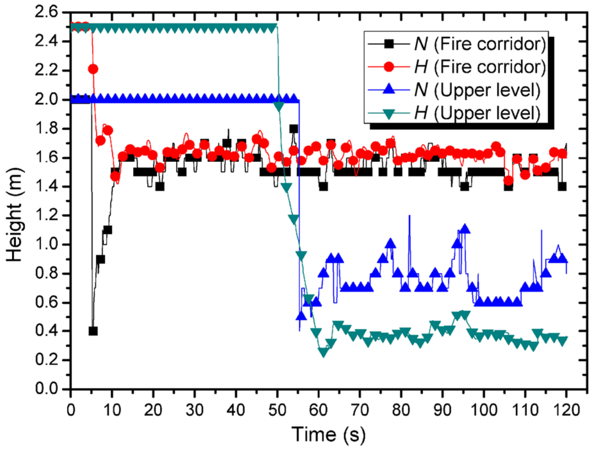

(a) Case 1-7

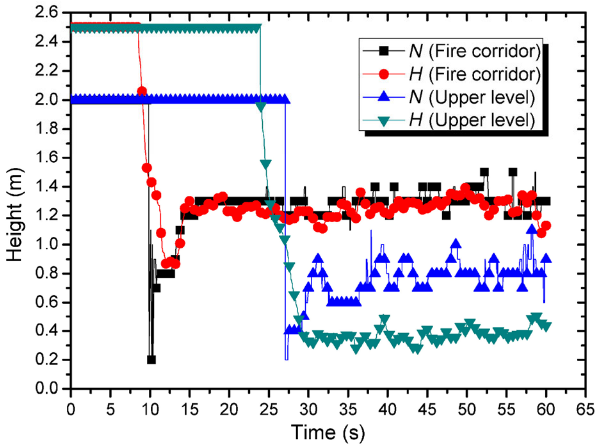

(b) Case 5-1

Fig. 4 Comparison of the smoke layer heights and the neutral plane heights (*N*: neutral plane height; *H*: smoke layer height)

Fig. 5 Smoke movement through the doors in the fire corridor and the upper level

in the upper level. Therefore, a temperature gradient exists along the entire height of the corridor. Figure 6 summarizes the general process of smoke propagation along the two-level corridor.

For corridors in underground buildings and other similar structures, the evacuation of personnel always follows the dispersal of smoke in the ceiling aperture, and the upper level is usually an important escape route. According to our simulation results, the upper level is filled with smoke in a short time, and the environment of the upper level was even more dangerous than that of the fire corridor. Therefore, preventing smoke from flowing out of the fire corridor through the ceiling aperture is crucial in reducing contaminated areas as well as quelling the fire loss, and thus deserves further study.

4.2 Smoke prevention at the ceiling aperture with counter airflow

Considering the need to manage smoke at the ceiling aperture of the fire corridor, smoke prevention with counter airflow was explored. Smoke can be prevented by the counter airflow when the inertial force of the airflow is sufficiently large to overcome smoke buoyancy. Therefore, the critical velocity of the counter airflow, which is defined as the minimum air velocity that is required to stop the outflowing of smoke, is an important parameter for measuring the effect of the counter airflow on smoke prevention and of main concern in this study. The critical velocities of the counter airflow in the ceiling aperture were obtained through numerical simulations of various fire scenarios. As mentioned previously, the ventilation rate was set sufficiently strong in the first simulation, and then gradually reduced until the critical velocity was obtained (Heskestad and Spaulding 1991). The direction of the velocity in the ceiling aperture was used as an indicator of the appearance of the critical velocity of the counter airflow.

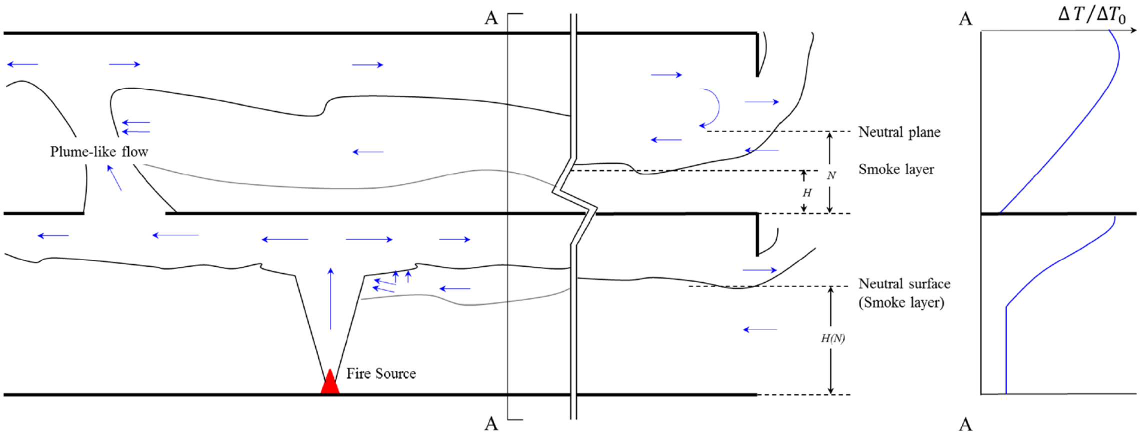

Fig. 6 Diagram of the smoke propagation and typical temperature profiles in the two-level corridor

Comparison of the temperature profiles for Case 5-6 with and without counter airflow (Fig. 7) shows that smoke was prevented from spreading through the ceiling aperture by a counter airflow at the critical velocity. However, the smoke layer is destroyed by the forced airflow in the fire corridor. The smoke layer height of the fire corridor in the cases with forced airflow was lower than that in corresponding cases without forced ventilation. Therefore, the effect of the counter airflow on the corridor environment needs comprehensive consideration before applying counter airflow measures.

The critical velocities of the counter airflow for different fire scenarios increase with HRR and decrease with fire–aperture distance, as shown in Fig. 8. The dependence of critical velocity on this distance becomes weak when the fire source was relatively far from the ceiling aperture.

The critical velocity of the counter airflow was analyzed using Froude modeling, which is usually adopted in these types of studies (Thomas 1968; Lee et al. 1979; Heskestad and Spaulding 1991; Williams et al. 1994). In the ideal case, the pattern of smoke movement is primarily affected by the buoyancy of smoke and the inertial forces of the airflow (Thomas 1968). The buoyancy is determined by the variation of density, and can be expressed as $\Delta\rho g h$. The inertial force of the counter airflow is assumed to be proportional to $\rho_0 V^2$. The Froude number, a dimensionless parameter, is defined as the ratio of the inertial force of the counter airflow and the buoyancy of smoke through the ceiling aperture. The fundamental assumption of Froude modeling is that the inertial force of the counter airflow and smoke buoyancy attains a balance at the critical condition at which smoke is halted. By substituting the density ratio with the temperature ratio according to the ideal gas equation, the critical Froude number is defined by (Heskestad and Spaulding 1991)

$$Fr_c = \frac{V_c}{\sqrt{2gh\frac{\Delta T}{T}}} \tag{5}$$

where V_c is the critical velocity of the counter airflow (m/s), g is the acceleration of gravity gravitational force (m/s^2), h is the characteristic length (m) taken as the height of the corridor for this study; ΔT and T are the temperature rise and the absolute temperature of the smoke through the ceiling aperture (K), respectively.

The critical velocity of the counter airflow can be characterized by the critical Froude number defined in

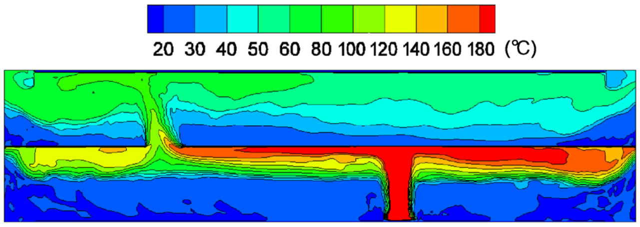

(a) Simulation without counter airflow (Case 5-6, fire corridor and upper level)

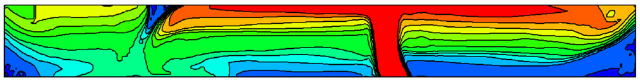

(b) Simulation of the critical velocity with counter airflow (Case 5-6, fire corridor)

Fig. 7 Temperature profiles for scenarios with and without counter airflow (Y=1.3 m)

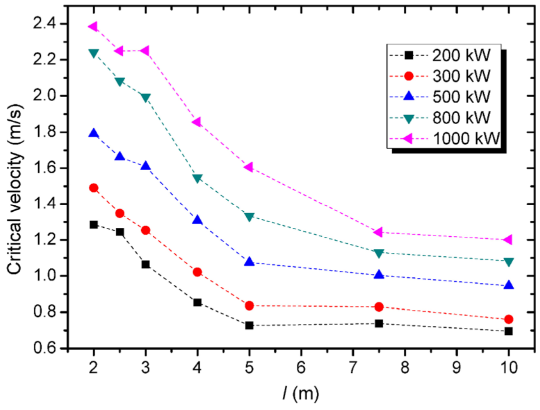

Fig. 8 Dependence on fire–aperture distance of the critical velocities for counter airflow for various heat release rates

Eq. (5). To analyze the effect of fire–aperture distance on the critical velocity of counter airflow, the distance between the fire source and the ceiling aperture was normalized by dividing the mean flame height, which is an important scaling parameter for fires (Zukoski 1986). The corresponding dimensionless distance is defined as

$$l^* = l / L \tag{6}$$

where l is the fire–aperture distance (m) and L is the mean height of the flame (m), which is calculated using formula (Heskestad 2002):

$$L = 0.235\dot{Q}^{2/5} - 1.02D \tag{7}$$

where $\dot{Q}$ is the HRR of fire (kW) and D is the diameter of fire source (m).

The critical Froude number and the dimensionless fire–aperture distance for all fire scenarios were calculated from simulation results, and illustrated in Fig. 9. Here, we propose a simple model for predicting the critical velocity of the counter airflow. Starting with

$$\begin{aligned} Fr_{\mathrm{c}} &= -0.14l^* + 0.80 \qquad l^* \leqslant 3.0 \\ Fr_{\mathrm{c}} &= 0.38 \qquad\qquad\quad\; l^* > 3.0 \end{aligned} \tag{8}$$

The variation of Fr_{c} with l^* divides into two regimes. In the first regime, Fr_{c} and l^* are linearly related, the slope and intercept being −0.14 and 0.80, respectively. In the second regime, the value of Fr_{c} is independent of l^* and remains at around 0.38. The critical value of l^* between the two regions is 3.0 (see Fig. 9), indicating that the ratio of the inertial force of the counter airflow and the buoyancy of smoke are independent if the fire–aperture distance in the corridor is three times as large as the mean flame height. The simple model may provide a rough guide in the design of counter airflow systems if used in preventing smoke from flowing out of the fire corridor through the ceiling aperture.

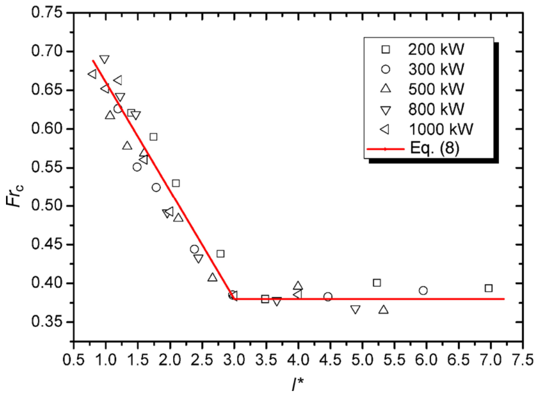

Fig. 9 Critical Froude number versus dimensionless fire–aperture distance for various heat release rates

5 Conclusions

Numerous CFD simulations were conducted using FDS to investigate the smoke propagation and management at the ceiling aperture in a two-level corridor model. The main conclusions are summarized as follows.

(1) Without smoke control measures, smoke spread quickly through the ceiling aperture of the fire corridor into the upper level. The smoke layer in the upper level almost descended to the floor at steady state through heat loss and backflow of the smoke caused by the doorway flow from the two ends of the upper corridor. The fire environment in the upper level was more dangerous than that in the fire corridor within a short time after the fire outbreak.

(2) Counter airflow is an effective way to prevent smoke from flowing out of the fire corridor through ceiling aperture into the corridor. Under the critical condition, smoke can be contained completely within the fire corridor, and contamination of the upper level avoided. However, the counter airflow can influence the smoke stability within the fire corridor.

(3) The critical velocity of the counter airflow was evaluated based upon Froude modeling. The critical Froude number initially declines linearly with dimensionless distance between fire source and ceiling aperture, and then becomes constant at about 0.38 with a dimensionless distance larger than 3.00.

Acknowledgements

The present work was supported by the Research Fund for the Doctoral Program of Higher Education of China (Grant Nos. 20123402110048 and 20123402120018) and the Anhui Provincial Natural Science Foundation (Grant No.1408085MKL94).

References

Bailey JL, Forney GP, Tatem PA, Jones, WW (2002). Development and validation of corridor flow submodel for CFAST. *Journal of Fire Protection Engineering*, 12: 139–161.

Chiu C-W, Chen C-H, Chen J-C, Shu C-M (2013). Analyses of smoke management models in TFT-LCD cleanroom. *Building Simulation*, 6: 403–413.

Chow WK (1996). Application of computational fluid dynamics in building services engineering. *Building and Environment*, 31: 425–436.

Chung KC, Tung HS, Wu YL (2005). Applied zone model to evaluate the smoke management in an underground structure. *Journal of Fire Sciences*, 23: 99–117.

Delichatsios MA (1981). The flow of fire gases under a beamed ceiling. *Combustion and Flame*, 43: 1–10.

Evers E, Waterhouse A (1978). A Complete Model for Analyzing Smoke Movement in Buildings. Building Research Establishment, UK.

Gong J, Li Y (2010). CFD modelling of the effect of fire source geometry and location on smoke flow multiplicity. *Building Simulation*, 3: 205–214.

Guo S, Yang R, Zhang H, Narayanan S, Atalla M (2009). Development of a fire zone model considering mixing behavior. *Journal of Thermophysics and Heat Transfer*, 23: 327–338.

Hadjisophocleous G, Jia Q (2009). Comparison of FDS prediction of smoke movement in a 10-storey building with experimental data. *Fire Technology*, 45: 163–177.

Havlovick BJ, Yadon JT, Farley JP, Williams FW (2002). Automated control of shipboard ventilation systems: Phase 2. Part A. Test results. Report, Naval Research Lab, Washington DC.

Heskestad G, Hill JP (1986). Experimental fires in multiroom/corridor enclosures. Gaithersburg, MD, USA: National Bureau of Standards.

Heskestad G, Spaulding RD (1991). Inflow of air required at wall and ceiling apertures to prevent escape of fire smoke. *Fire Safety Science*, 3: 919–928.

Heskestad G (2002). Fire plumes, flame height, and air entrainment. In: The SFPE Handbook of Fire Protection Engineering, 3rd edn. Quincy, MA, USA: National Fire Protection Association.

Hu L, Wu L, Lu K, Zhang X, Liu S, Qiu Z (2014). Optimization of emergency ventilation mode for a train on fire stopping beside platform of a metro station. *Building Simulation*, 7: 137–146.

Hu LH, Huo R, Li YZ, Wang HB, Chow WK (2005). Full-scale burning tests on studying smoke temperature and velocity along a corridor. *Tunnelling and Underground Space Technology*, 20: 223–229.

Hu LH, Li YZ, Huo R, Yi L, Chow WK (2006a). Full-scale experimental studies on mechanical smoke exhaust efficiency in an underground corridor. *Building and Environment*, 41: 1622–1630.

Hu LH, Huo R, Peng W, Chow WK, Yang RX (2006b). On the maximum smoke temperature under the ceiling in tunnel fires. *Tunnelling and Underground Space Technology*, 21: 650–655.

Hu LH, Fong NK, Yang LZ, Chow WK, Li YZ, Huo R (2007). Modeling fire-induced smoke spread and carbon monoxide transportation in a long channel: Fire dynamics simulator comparisons with measured data. *Journal of Hazardous Materials*, 140: 293–298.

Hu LH, Peng W, Huo R (2008). Critical wind velocity for arresting upwind gas and smoke dispersion induced by near-wall fire in a road tunnel. *Journal of Hazardous Materials*, 150: 68–75.

Hua J, Wang J, Kumar K (2005). Development of a hybrid field and zone model for fire smoke propagation simulation in buildings. *Fire Safety Journal*, 40: 99–119.

Hwang CC, Edwards JC (2005). The critical ventilation velocity in tunnel fires—A computer simulation. *Fire Safety Journal*, 40: 213–244.

Ingason H, Werling P (2002). Experimental study of inlet openings in multi-story underground construction. *Journal of Fire Protection Engineering*, 12: 79–92.

Gottuk D T, Mealy C, Floyd J (2008). Smoke transport and FDS validation. *Fire Safety Science*, 9: 129–140.

Kim MB, Han YS, Yoon MO (1998). Laser-assisted visualization and measurement of corridor smoke spread. *Fire Safety Journal*, 31: 239–251.

Kunsch JP (1998). Critical velocity and range of a fire-gas plume in a ventilated tunnel. *Atmospheric Environment*, 33: 13–24.

Lee CK, Chaiken RF, Singer JM (1979). Interaction between duct fires and ventilation flow: An experimental study. *Combustion Science and Technology*, 20: 59–72.

Lee SR, Ryou HS (2006). A numerical study on smoke movement in longitudinal ventilation tunnel fires for different aspect ratio. *Building and Environment*, 41: 719–725.

Matsuyama K, Mizuno M, Wakamatsu T, Harada K (2001). A systematic experiments of room and corridor smoke filling for use in calibration of zone and CFD fire models for engineering fire safety design of buildings. *Fire Science and Technology*, 21: 43–55.

McGrattan KB, Hostikka S, Floyd JE (2010). Fire Dynamics Simulator (Version 5), User's Guide. Gaithersburg, MD, USA: NIST Special Publication.

Mowrer F (2002). Enclosure smoke filling and management with mechanical ventilation. *Fire Technology*, 38: 33–56.

Oka Y, Atkinson GT (1995). Control of smoke flow in tunnel fires. *Fire Safety Journal*, 25: 305–322.

Quintiere JG, McCaffrey BJ, Rinkinen W (1978). Visualization of room fire induced smoke movement and flow in a corridor. *Fire and materials*, 2: 18–24.

Roh JS, Ryou HS, Kim DH, Jung WS, Jang YJ (2007). Critical velocity and burning rate in pool fire during longitudinal ventilation. *Tunnelling and Underground Space Technology*, 22: 262–271.

Thomas PH (1968). The Movement of Smoke in Horizontal Passages Against an Air Flow. BRE Trust. Fire Research Station.

Wang L, Lim J, Quintiere JG (2011). On the prediction of fire-induced vent flows using FDS. *Journal of Fire Sciences*, 30: 110–121.

Williams FW, Forssell EW, DiNenno PJ, Beyler CL, Lain P (1994). Shipboard smoke control tests using forced counterflow air supply. Report, Naval Research Lab, Washington DC.

Wu Y, Bakar MZA (2000). Control of smoke flow in tunnel fires using longitudinal ventilation systems—A study of the critical velocity. *Fire Safety Journal*, 35: 363–390.

Wu Y, Li A, Ma J, Gao R, Hu J, Xiao B, Zhang P (2013). Numerical studies on smoke natural filling in an underground passage with validation by reduced-scale experiments. *Nature Environment and Pollution Technology*, 12: 35-42.

Zhong MH, Li PD, Liu TM, Wei X, Liao GX (2005). Experimental study on fire smoke movement in a multi-floor and multi-room building. *Science in China Series E: Engineering & Materials Science*, 48: 292–304.

Zhu X (2009). Hybrid model for smoke and heat propagation in complex structures. PhD Thesis, Carleton University, Canada.

Zukoski EE (1986). Fluid dynamic aspects of room fires. Paper presented in Proceedings of 1st International Symposium on Fire Safety Science.